Articles

Thermodynamics of the Hydrothermal Synthesis of Calcium Titanate with Reference to Other Alkaline-Earth Titanates

Malgorzata M. Lencka and Richard E. Riman*

Department of Ceramics, College of Engineering, Rutgers, The State University of New Jersey, Piscataway, New Jersey 08855-0909

Received May 24, 1994. Revised Manuscript Received September 22, 1994[⊗]

A thermodynamic model for hydrothermal synthesis of alkaline-earth titanates has been utilized to predict the optimum conditions for the synthesis of phase-pure $CaTiO_3$. The predictions have been experimentally validated using $Ca(NO_3)_2$ or $Ca(OH)_2$ as sources of calcium and crystalline or hydrous TiO_2 as a source of titanium at moderate temperatures (433-473 K). Practical experimental techniques have been developed to avoid the contamination of the calcium titanate with undesirable solid phases (e.g., calcium carbonate or hydroxide). These conditions were compared with those previously determined for the Ba-Ti and Sr-Ti hydrothermal systems.

Introduction

Hydrothermal media provide an effective reaction environment for the synthesis of numerous ceramic materials. In particular, phase-pure ceramic powders can be hydrothermally synthesized in a single experimental step from simple and inexpensive precursors at moderate temperatures and pressures.[1-4] To take advantage of the opportunities offered by hydrothermal synthesis, it is important to select a precursor system that is both reactive and cost effective. However, the reactivity of a precursor system can be judged only by optimizing the processing variables such as reagent concentration, pH, temperature, and pressure, which can be extremely time consuming due to the large number of variables involved. To improve the efficiency of evaluating the precursor system, Lencka and Riman[2-4] proposed a comprehensive thermodynamic model that simulates hydrothermal reactions. The predictions of the model have been confirmed experimentally for the syntheses of $BaTiO_3$,[2,4] $PbTiO_3$,[3] and $SrTiO_3$.[4] In this study we utilize this model to predict the optimum conditions for the synthesis of $CaTiO_3$ and compare them with those previously determined for the other alkaline-earth titanates, $SrTiO_3$ and $BaTiO_3$.

Crystalline $CaTiO_3$ has been previously obtained by Kutty and Vivekanandan[5] at temperatures from 423 to 473 K, using CaO and TiO_2 gel as starting materials. The TiO_2 gel ($TiO_2 \cdot xH_2O$) was obtained by hydrolyzing $TiOCl_2$ with NH_3(aq) and CaO was prepared by decomposing $CaAc_2$ at ca. 973 K. Excess Ca in the reaction products was removed by washing with dilute acetic acid solutions. In a separate study, Kutty and Vivekanandan[6] hydrothermally synthesized $CaTiO_3$ from freshly precipitated hydrothermal TiO_2 (rutile) and CaO as starting materials at temperatures greater than 513 K. However, the synthesis was incomplete even at 553 K when hydrothermal TiO_2 (anatase) was used. These results could be attributed to inappropriate reaction conditions and/or sluggish reaction kinetics. The objective of our work is to use thermodynamic modeling to resolve these issues and use the model to design an efficient synthesis route to prepare phase-pure $CaTiO_3$ with inexpensive precursors at minimal temperatures.

Theoretical Predictions

The theoretical model for simulating hydrothermal reactions in multicomponent aqueous systems has been described in detail in a previous paper.[2] The model is based on the knowledge of standard-state properties of all species that may exist in the system coupled with a comprehensive activity coefficient model for those species which may exist in the aqueous phase. Thus, the application of the model to a particular system necessitates the knowledge of the standard Gibbs energies ΔG_f°, enthalpies ΔH_f° of formation and entropies S° at a reference temperature (298.15 K) as well as partial molar volumes V° and heat capacities C_p° as functions of temperature. Table 1 lists these properties for the species that may exist in significant quantities in the Ca-Ti hydrothermal system. Since atmospheric carbon dioxide can play a role in the synthesis, data for CO_2-derived species are also given in Table 1.

The model is used to calculate the equilibrium concentrations of all, solid and aqueous, species in the

[⊗] Abstract published in *Advance ACS Abstracts,* November 1, 1994.

(1) Dawson, W. *Ceram. Bull.* **1988**, *67*, 1673.
(2) Lencka, M. M.; Riman, R. E. *Chem. Mater.* **1993**, *5*, 61.
(3) Lencka, M. M.; Riman, R. E. *J. Am. Ceram. Soc.* **1993**, *76*, 2649.
(4) Lencka, M. M.; Riman, R. E. *Ferroelectrics* **1994**, *151*, 159.
(5) Kutty, T. R. N.; Vivekanandan, R. *Mater. Lett.* **1987**, *5*, 79.
(6) Kutty, T. R. N.; Vivekanandan, R. *Mater. Chem. Phys.* **1988**, *19*, 533.
(7) Eckert, J., Jr.; Hung-Houston, C. C.; Gersten, B. L.; Lencka, M. M.; Riman, R. E., manuscript in preparation.
(8) Limar, T. F.; Chereduichenko, I. F.; Sverdlova, A. N.; Velichko, Yu. N.; Barabanshchikova, R. M. Translated from: *Izv. Akad. Nauk SSSR, Neorg. Mater.* **1970**, *6*, 1829.

0897-4756/95/2807-0018$09.00/0

Table 1. Standard-State Properties of Individual Species in the Ca–Ti–CO_2 Hydrothermal System

ionic species	H^+	Ca^{2+}	$CaOH^+$	$CaHCO_3^+$	HCO_3^-	CO_3^{2-}
$\Delta G_f°$ (kJ·mol^{-1})	0	−552.790	−717.138	−1145.705	−586.940	−527.983
$\Delta H_f°$ (kJ·mol^{-1})	0	−543.083	−764.417	−1231.560	−689.933	−675.23
$S°$ (J·mol^{-1}·K^{-1})	0	−56.484	−14.468	66.944	98.45	−50.00
$C_p°$ (J·mol^{-1}·K^{-1})	0	−31.506	105.604		−35.4	−290.8
$10^6V°$ (m^3·mol^{-1})		−18.06	−1.58	9.55	24.6	−5.02
refs	15	12, 13	17, 18[c]	12	12, 13	12, 13

ionic species	OH^-	Ti^{4+}	$TiOH^{3+}$	$Ti(OH)_2^{2+}$	$Ti(OH)_3^+$	$HTiO_3^-$
$\Delta G_f°$ (kJ·mol^{-1})	−157.30	−354.18	−614.00	−869.56	−1092.5	−955.88
$\Delta H_f°$ (kJ·mol^{-1})	−230.03					
$S°$ (J·mol^{-1}·K^{-1})	−10.71	−456.5	−189.5	−40.8	56.9	117.3
$C_p°$ (J·mol^{-1}·K^{-1})	−137.2					
$10^6V°$ (m^3·mol^{-1})	−4.18					
refs	13, 18	17, 13	17, 19[c]	17, 19[c]	17, 19[c]	20

ionic species	NO_3^-	K^+	Na^+
$\Delta G_f°$ (kJ·mol^{-1})	−110.91	−282.46	−261.88
$\Delta H_f°$ (kJ·mol^{-1})	−206.81	−252.17	−240.30
$S°$ (J·mol^{-1}·K^{-1})	146.9	101.0	58.41
$C_p°$ (J·mol^{-1}·K^{-1})	−68.6	8.28	37.9
$10^6V°$ (m^3·mol^{-1})	29.0	9.06	−1.11
refs	12, 13	12, 13	12, 13

aqueous species	H_2O	$Ca(OH)_2$	$CaCO_3$	CO_2	$Ti(OH)_4$	HNO_3
$\Delta G_f°$ (kJ·mol^{-1})	−237.141	−867.246	−1099.76	−385.97	−1318.4	−103.47
$\Delta H_f°$ (kJ·mol^{-1})	−285.830	−1003.03	−1202.44	−413.80	−1511.3	−190.00
$S°$ (J·mol^{-1}·K^{-1})	69.950	−78.00	10.46	117.6	54.8	178.7
$C_p°$ (J·mol^{-1}·K^{-1})	75.288			243.1	50.2	75.3
$10^6V°$ (m^3·mol^{-1})	18.07	−1.65	−14.4	32.8		
refs	15, 10	15	12	12, 14, 18	17	12, 14, 18

solid species[a]	CaO	$Ca(OH)_2$	$CaCO_3$	$CaTiO_3$	$Ca_3Ti_2O_7$	$Ca_4Ti_3O_{10}$	TiO_2
$\Delta G_f°$ (kJ·mol^{-1})	−603.509	−898.470	−1129.178	−1575.247	−3751.008	−5386.854	−890.702
$\Delta H_f°$ (kJ·mol^{-1})	−635.089	−986.085	−1207.302	−1660.596	−3950.499	−5671.663	−946.007
$S°$ (J·mol^{-1}·K^{-1})	38.074	83.387	92.676	93.638	234.701	328.444	50.292
$C_p°$ (J·mol^{-1}·K^{-1})	42.122	87.487	81.873	97.649	239.315	337.809	55.103
a (J·mol^{-1}·K^{-1})	49.604	103.226	104.516	127.441	298.964	424.050	62.820
10^3b (J·mol^{-1}·K^{-2})	5.1429	15.767	21.924	5.6890	15.899	21.588	11.383
$10^{-5}c$ (J·mol^{-1}·K)	−8.0187	−18.137	−25.941	−27.992	−57.238	−82.384	−9.8968
$10^6V°$ (m^3·mol^{-1})	16.764	33.056	36.934	33.16			18.82
refs	10, 16	10, 16	12, 16	10, 16	10	10	10, 16

solid species[a]	$Ca(NO_3)_2$	$Ca(NO_3)_2·2H_2O$	$Ca(NO_3)_2·3H_2O$	$Ca(NO_3)_2·4H_2O$	NaOH	KOH
$\Delta G_f°$ (kJ·mol^{-1})	−742.053	−1229.019	−1471.567	−1713.076	−379.737	−378.86
$\Delta H_f°$ (kJ·mol^{-1})	−938.392	−1540.758	−1838.002	−2132.330	−425.931	−424.68
$S°$ (J·mol^{-1}·K^{-1})	193.301	269.399	319.201	375.301	64.434	78.91
$C_p°$ (J·mol^{-1}·K^{-1})	149.364	231.496	267.060	300.532	59.570	64.897
a (J·mol^{-1}·K^{-1})	122.883	205.018	240.582	274.054	36.666	42.857
10^3b (J·mol^{-1}·K^{-2})	154.011	154.011	154.011	154.011	75.175	73.397
$10^{-5}c$ (J·mol^{-1}·K)	−17.281	−17.281	−17.281	−17.281	0	0
$10^6V°$ (m^3·mol^{-1})	66.09	98.581		123.64	18.78	27.45
refs	10, 16	10, 11	10	10, 11	10, 16	10, 16

gaseous species[b]	H_2O	HNO_3	CO_2
$\Delta G_f°$ (kJ·mol^{-1})	−228.586	−74.848	−394.358
$\Delta H_f°$ (kJ·mol^{-1})	−241.826	−134.976	−393.509
$S°$ (J·mol^{-1}·K^{-1})	188.835	266.90	213.737
$C_p°$ (J·mol^{-1}·K^{-1})	33.609	54.225	37.149
a (J·mol^{-1}·K^{-1})	32.074	11.541	44.225
10^3b (J·mol^{-1}·K^{-2})	3.2165	174.64	8.786
$10^{-5}c$ (J·mol^{-1}·K)	0	0	−8.619
10^5d (J·mol^{-1}·K^{-3})	0.6794	−10.866	0
T_c (K)	647.3	520.0	304.1
P_c (bar)	221.2	68.90	72.78
ω	0.344	0.714	0.231
refs	15, 18, 21	12, 18, 21	12, 21

[a] Heat capacities are calculated from the relation $C_p° = a + bT + cT^{-2}$. [b] Heat capacities are calculated from the relation $C_p° = a + bT + cT^{-2} + dT^2$. [c] Estimated.

system for different synthesis conditions. The equilibrium concentrations have been utilized to construct stability diagrams that show the predominant species as a function of pH of the solution and the total molality of an aqueous precursor. The total molality of the aqueous metal precursor (m_{Me_T}) refers to the equilibrium concentration of all dissolved metal species and does not include those compounds that precipitate from the solution. The curved lines on the stability diagram correspond to the states of incipient precipitation of solid

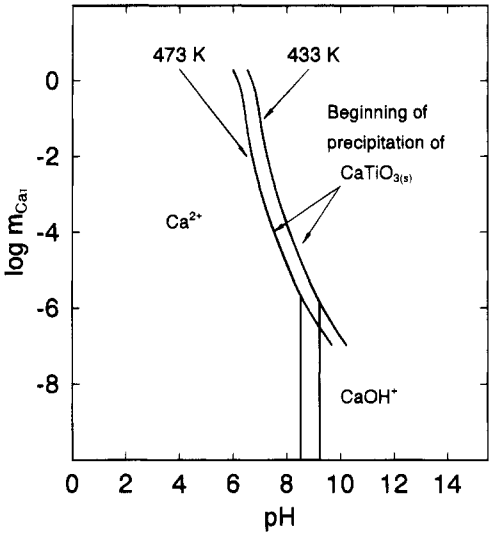

Figure 1. Calculated phase stability diagram for the hydrothermal system Ca–Ti at 433 and 473 K for the stoichiometric molar ratio of Ca and Ti precursors (Ca/Ti = 1).

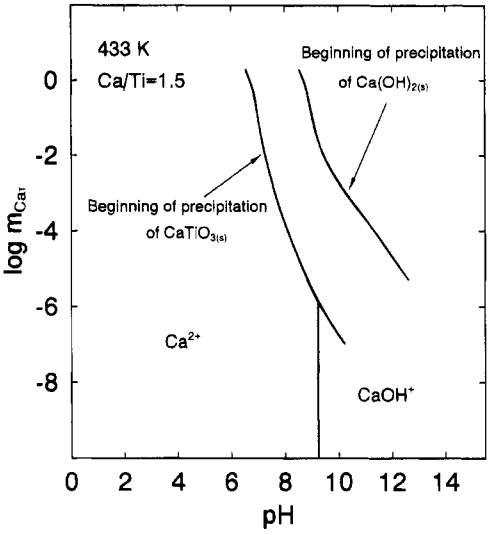

Figure 2. Calculated phase stability diagram for the hydrothermal system Ca–Ti at 433 K for the nonstoichiometric molar ratio of Ca and Ti precursors (Ca/Ti = 1.5).

components, such as $CaTiO_3$. On the other hand, the vertical straight lines correspond to the loci where two aqueous species have equal concentrations. These loci are independent of molality over a limited molality range. They are shown only in the region of the diagram where solid phases do not precipitate. In principle, they could be extended into the solid–liquid region. However, they would have to be terminated at some point at which all calcium precipitates from the solution. The location of this point will depend not on the total molality of calcium in the solution (m_{Ca_T}) but on the input amount of calcium ($m_{Ca_{IN}}$). Therefore, the extensions of the vertical lines into the solid–liquid region are not plotted in the stability diagrams.

Figure 1 shows the stability diagram for the Ca–Ti hydrothermal system at two temperatures (433 and 473 K) when the input concentrations of calcium and titanium precursors are equal, i.e., the molar Ca/Ti ratio is equal to 1. The condition of Ca/Ti = 1 corresponds to the composition of the desired product $CaTiO_3$. The stability diagram is, in general, not affected by the chemical identity of the Ca and Ti precursors provided that they do not introduce any complex species. As shown in Figure 1, the precipitation of $CaTiO_3$ at 433 K begins at pH values ranging from 6.5 to 10.2, depending on the concentration of Ca in the aqueous phase. Temperature has only a small effect on altering the precipitation conditions for $CaTiO_3$. For instance, an increase in temperature by 40 degrees shifts the equilibrium pH downwards by about 0.6 pH units.

Figure 2 shows what may happen in the system at T = 433 K when the molar ratio Ca/Ti is greater than 1, i.e., when an excess amount of calcium is present. The calculations were performed for the Ca/Ti ratio equal to 1.5. In that case, $CaTiO_3$ will be the first solid phase to precipitate from the solution. $CaTiO_3$ is the only phase containing both Ca and Ti that can precipitate from the Ca–Ti hydrothermal system. Other multicomponent oxides containing Ca and Ti (e.g., $Ca_4Ti_3O_{10}$ and $Ca_3Ti_2O_7$) do not precipitate from the solution. Also, no experimental data indicate the formation of multicomponent oxides other than $CaTiO_3$ in hydrothermal solutions. The remainder of Ca may precipitate as $Ca(OH)_2$ because calcium hydroxide becomes stable at still higher pH values as shown in Figure 2. These results indicate that practical syntheses should be performed with the molar Ca/Ti ratio equal to 1.

While the stability diagrams provide information about the conditions of incipient precipitation of various solid phases, they do not specify the reaction conditions required for precipitation of a phase-pure product. To accomplish this goal, a yield diagram should be consulted. In contrast to the stability diagrams, the yield diagrams are shown with the total input concentration of the metal ($m_{Me_{IN}}$) as the independent variable instead of the equilibrium concentration of all dissolved species. The input concentration of the metal is equal to the initial concentration of the metal (Me) precursor. As a result of the reaction, the metal (Me) can be converted to the desired product $MeTiO_3$ with a certain yield while the reminder of the Me precursor can remain in the solution. For the purpose of yield analysis, it is necessary to use the input concentration because we are concerned not only with the equilibrium concentration of species in saturated solution but also with the conversion of the precursor into the desired product. At the solubility curve (shown in both stability and yield diagrams), the yield is very small because the solubility curve corresponds to incipient precipitation of the desired product. The yield increases as we move beyond the solubility curve into the solid–liquid region and, finally, reaches at least 99.995% in the shaded area. Figures 3 and 4 provide direct guidance for the experimental synthesis because they indicate that phase-pure $CaTiO_3$ can be obtained only within the shaded area of the yield diagram. Figures 3 and 4 show the yield diagrams for $Ca(NO_3)_2$ (dashed line) or $Ca(OH)_2$ and TiO_2 as precursors at temperatures of 433 and 473 K, respectively. $Ca(NO_3)_2$ and $Ca(OH)_2$ have been chosen as the simplest, water-soluble sources of calcium. As shown in Figures 3 and 4, the region of complete yield of $CaTiO_3$ (yield greater than 99.995%) is much smaller than the $CaTiO_3$ stability range. The complete yield region starts at pH values greater by ca. 2–3 than those corresponding to the beginning of precipitation. Pure $CaTiO_3$ can be obtained only when the input molal concentration of Ca is greater than ca. 5×10^{-5} mol/kg

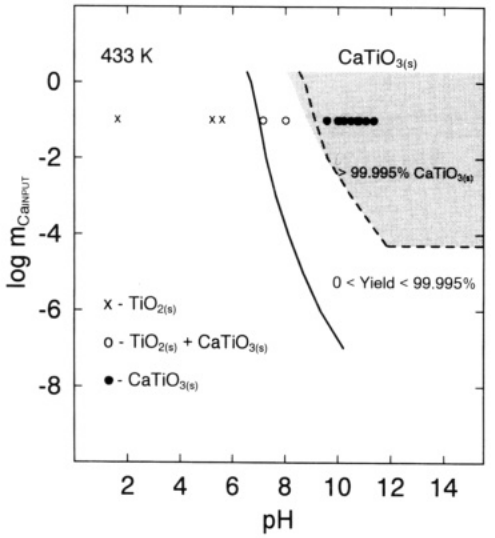

Figure 3. Calculated yield diagram for the hydrothermal synthesis of $CaTiO_3$ at 433 K from $Ca(NO_3)_2$ (dashed line) or $Ca(OH)_2$ and TiO_2 as precursors. Symbols (×, ○, ●) denote the conditions of experimental syntheses performed.

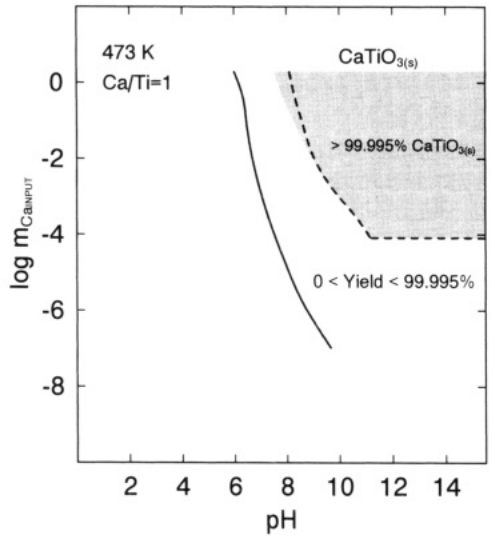

Figure 4. Calculated yield diagram for the hydrothermal synthesis of $CaTiO_3$ at 473 K from $Ca(NO_3)_2$ (dashed line) or $Ca(OH)_2$ and TiO_2 as precursors.

at $T = 433$ K and 8×10^{-5} mol/kg at $T = 473$ K. The difference between the yield diagrams (cf. Figures 3 and 4) with $Ca(NO_3)_2$ (dashed line) and $Ca(OH)_2$ as precursors is significant only at relatively high input molal concentrations of Ca, i.e., above ca. 10^{-2} mol/kg. The area of the $CaTiO_3$ yield greater than 99.995% is somewhat larger in this region when $Ca(OH)_2$ is used as a precursor. Thus, unlike stability diagrams, the yield diagrams are somewhat sensitive to the chemical identity of precursors. This results from the fact that different amounts of OH^- ions are consumed in the reaction, depending on the chemical identity of the precursor.

To maintain the correct pH of the hydrothermal system, it is necessary to use alkaline mineralizers (i.e., pH adjusting agents). NaOH and KOH are most convenient for this purpose. The minimum amounts of the mineralizer that are necessary to obtain $CaTiO_3$ at 433 K with a yield greater than 99.995% are given in Table 2 for different input molalities of calcium precursors. As expected, these amounts strongly depend on

Table 2. Minimum Molalities of Mineralizer (KOH or NaOH) Needed To Obtain $CaTiO_3$ with a Yield Greater Than 99.995% at 433 K

	$m_{Ca_{IN}}$					
	0.0001	0.001	0.01	0.1	1.0	2.0
from $Ca(OH)_2$ and TiO_2	1.75	0.14	0.012	0.002	0.0	0.0
from $Ca(NO_3)_2$ and TiO_2	1.68	0.14	0.04	0.21	2.0	4.0

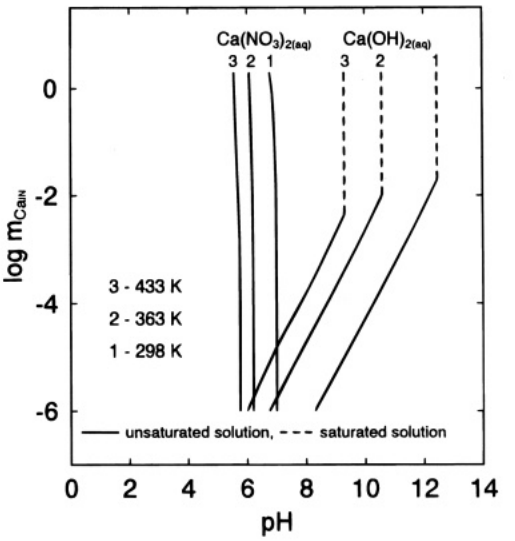

Figure 5. Solution pH resulting from the dissolution of calcium precursors: $Ca(OH)_2$ and $Ca(NO_3)_2$ in water at 298, 363, and 433 K.

the alkalinity of the calcium precursor. If calcium hydroxide is used as a precursor and its concentration is reatively high (greater than 0.1), practically no mineralizer is necessary. In contrast, significant amounts of mineralizer are needed when a non-alkaline precursor, $Ca(NO_3)_2$, is used. However, the mineralizer is always necessary if the synthesis is performed in very dilute solutions.

The practical synthesis of $CaTiO_3$ can be affected by the presence of atmospheric carbon dioxide which may lead to the formation of undesirable carbonates. Unless the system is isolated from the atmosphere, contact with CO_2 may occur during precursor solution preparation and/or from an atmospheric contaminant inside the autoclave. The former effect is due to the alkalinity of the calcium precursor solution. For instance, solutions of $Ca(OH)_2$ are moderately alkaline whereas solutions of $Ca(NO_3)_2$ are nearly neutral. This is illustrated in Figure 5 which shows the pH of solutions obtained by dissolving various amounts ($m_{Ca_{IN}}$) of $Ca(NO_3)_2$ or $Ca(OH)_2$ in water at three different temperatures. $Ca(NO_3)_2$ and $Ca(OH)_2$ were the only solutes considered in this case. For those solutions that are alkaline, absorption of CO_2 leads to the formation of carbonates. To illustrate this effect, the weight percentage loss of soluble calcium due to the formation of $CaCO_3$ was calculated for a $Ca(OH)_2$ solution in contact with an infinite reservoir of air with the mole fraction of CO_2 equal to 3.31×10^{-4}. As shown in Table 3, the formation of carbonates becomes important when the concentration of $Ca(OH)_2$ is greater than ca. 5.0×10^{-4} mol/kg at 298 K and greater than 10^{-4} mol/kg at 363 K. When the calcium concentration is higher than 10^{-2} mol/kg, practically all calcium converts to $CaCO_3$. These results indicate that the contact with atmosphere should be avoided during the preparation of the solutions for

Table 3. Relative Amount of Calcium Precipitated as $CaCO_3$ from the $Ca(OH)_2$ Solution in an Air Atmosphere ($y_{CO_2} = 3.31 \times 10^{-4}$)

$m_{Ca_{IN}}$	mol % $CaCO_3$ (298 K)	mol % $CaCO_3$ (363 K)
10^{-5}	0.0	0.0
10^{-4}	0.0	0.0
1.9×10^{-4}	0.0	3.7
5.1×10^{-4}	0.6	64.1
5.2×10^{-4}	2.5	64.8
10^{-3}	49.3	81.7
10^{-2}	94.9	98.2
10^{-1}	99.5	99.8

hydrothermal synthesis. This is also the case when $Ca(NO_3)_2$ is used as precursor in conjunction with NaOH or KOH as mineralizers because the presence of the mineralizers makes the solutions alkaline.

However, when CO_2 exposure is permitted only during the hydrothermal reaction stage, carbonate formation is not a concern. For instance, carbonate formation was simulated for the Ca–Ti hydrothermal system confined in a typical autoclave with 40 cm^3 of its volume filled with CO_2-containing air. In this case no formation of carbonates was detected.

The effect of atmospheric CO_2 on the purity of the final product is different for the Ca–Ti, Sr–Ti, and Ba–Ti hydrothermal systems. It is directly correlated with the alkalinities of Ca, Sr, and Ba because the absorption of CO_2 is facilitated by the alkalinity of the solution. Accordingly, the metal concentration thresholds above which carbonates precipitate are different for the three systems. In the case of Ca–Ti hydrothermal system, the contact with an infinite reservoir of CO_2-containing air at $T = 298$ K leads to the contamination with carbonates when the concentration of Ca is greater than 5.0×10^{-4} m. Since Sr and Ba are more alkaline, this threshold is 8.9×10^{-5} m for the Sr–Ti system and only 1.1×10^{-5} m for the Ba–Ti system. In the case of the Ba–Ti hydrothermal system, carbonates can precipitate even in a closed system containing a small amount of CO_2-containing air in an autoclave.[2]

It is worthwhile to compare the conditions for the synthesis of the alkaline-earth titanates, $CaTiO_3$, $SrTiO_3$, and $BaTiO_3$. The syntheses of $SrTiO_3$ and $BaTiO_3$ were discussed in detail in previous papers.[2,4] Figure 6 shows the calculated phase stability diagrams for three hydrothermal systems Ca–Ti, Sr–Ti, and Ba–Ti at 433 K. The diagrams are qualitatively similar because of the chemical similarity of the Ca, Sr, and Ba cations. The incipient precipitation lines of $CaTiO_3$ and $SrTiO_3$ are very close to each other. The $BaTiO_3$ line is located at somewhat higher alkalinities. Its distance from the $SrTiO_3$ line is about 1.2 pH unit. The relative location of the incipient precipitation lines is a result of an interplay of several independent factors. Among them, most important are the relative magnitudes of standard-state thermodynamic functions, alkalinity of the Ba, Sr, and Ca species as well as specific interactions between ions that determine the activity coefficients. It is apparent that the incipient precipitation line for the titanate of the most alkaline metal, i.e., Ba lies at higher pH values. The differences between the $CaTiO_3$ and $SrTiO_3$ lines become visible only at relatively high and small (but not intermediate) concentrations. The $CaTiO_3$ and $SrTiO_3$ lines cross each other.

Figure 7 compares the yield diagrams calculated for

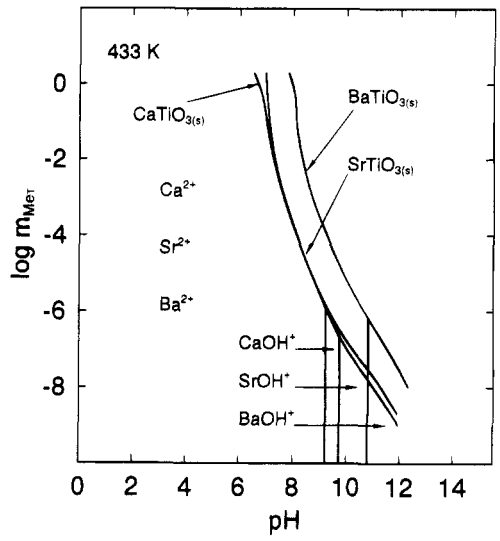

Figure 6. Comparison of calculated phase stability diagrams for the hydrothermal systems Ca–Ti, Sr–Ti, and Ba–Ti at 433 K for the stoichiometric molar ratios of precursors.

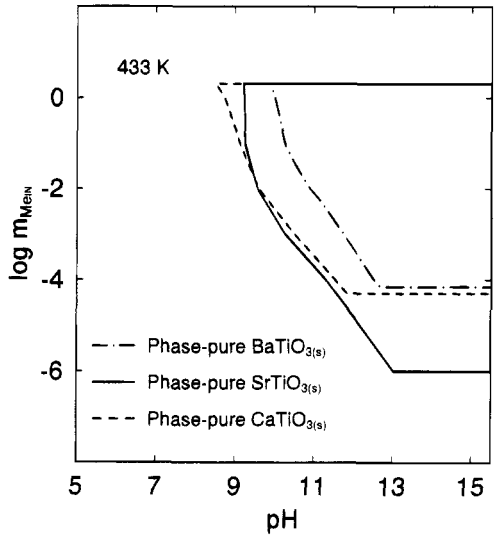

Figure 7. Comparison of calculated yield diagrams for the hydrothermal syntheses of $CaTiO_3$, $SrTiO_3$, and $BaTiO_3$ at 433 K from TiO_2 and alkaline-earth nitrates as precursors.

the syntheses of $CaTiO_3$, $SrTiO_3$, and $BaTiO_3$ from alkaline-earth nitrates and TiO_2 at 433 K. Phase-pure $MeTiO_3$ can be obtained at input molalities of Ba, Sr and Ca greater than 7×10^{-5}, 10^{-6}, and 5×10^{-5}, respectively. Otherwise, the relative location of the 99.995% yield regions for the three titanates is similar to the pattern noted for stability diagrams.

Finally, it is worthwhile to compare the amounts of the mineralizer that are necessary to obtain phase-pure $MeTiO_3$. Figure 8 shows this comparison at 433 K. For relatively high input molal concentrations of the metal precursor ($m_{Me_{IN}} > 0.1$ mol/kg) the amounts of the mineralizer are practically the same for all metals (Ca, Sr, and Ba). This is because in concentrated solutions the consumption of OH^- ions is caused by the following predominant reaction:

$$Me^{2+} + TiO_2 + 2OH^- = MeTiO_3 + H_2O$$

Thus, 2 mol of OH^- is consumed for the synthesis of 1 mol of $MeTiO_3$, and only a relatively small amount of

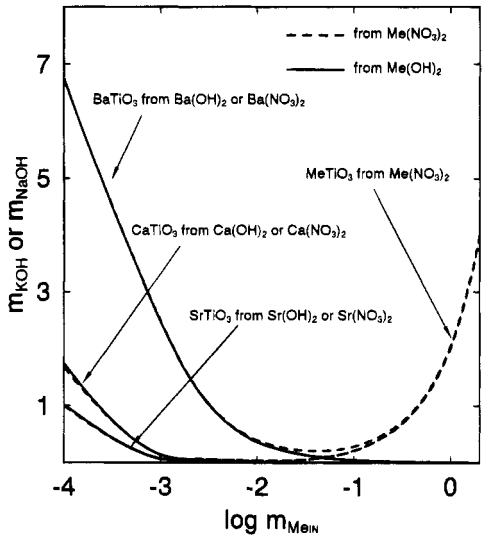

Figure 8. Equilibrium mineralizer concentrations needed to obtain phase-pure alkaline-earth titanates at 433 K.

OH^- is necessary to ensure the correct pH for each respective alkaline earth. Unlike the syntheses with nitrates, the use of metal hydroxide precursors at high concentrations does not require the addition of mineralizer because the necessary concentration of OH^- groups is readily provided by the hydroxide precursor. In contrast, at dilute concentrations identical amounts of mineralizer are needed irrespectively of whether a nitrate or a hydroxide is used as a precursor. However, the required mineralizer concentration differs substantially for the three metals. This may be caused by the strongly specific effects of the chemical identity of cations on activity coefficients due to the high concentration of mineralizer required to effect a complete reaction to form alkaline-earth titanates.

Experimental Procedure

To verify the theoretical predictions for $CaTiO_3$ formation, syntheses were performed using $Ca(NO_3)_2$ and $Ca(OH)_2$ as sources of calcium. Commercial anhydrous TiO_2 or freshly prepared hydrous gel $TiO_2 x H_2O$ were used as a source of titanium. $Ca(NO_3)_2 4H_2O$ (Fisher Scientific, Fair Lawn, NJ, >99.2%), $Ca(OH)_2$ (Johnson Matthey, Alfa Aesar, Ward Hill, MA, >98.8%) were used as sources of calcium. Anhydrous TiO_2 powder (P25, Degussa, Dublin, OH, 85 vol % of anatase) and hydrous TiO_2 gel obtained by hydrolyzing $Ti(i\text{-}OC_3H_7)_4$ (Aldrich Chemical Co., Inc., Milwaukee, WI) at room temperature[3] were also used. Solution pH was adjusted using KOH (Aldrich, 99.99%) or NaOH (Aldrich, 99.99%). The reagents were charged into 125 mL stainless steel Teflon-lined autoclaves (acid digestion bombs: Parr Instrument Co., Moline, IL) along with deionized water (10 MΩ cm, Millipore Corp., Bedford, MA). Syntheses were performed with the molar ratio Ca/Ti equal to 1 using the input molality of $Ca(NO_3)_2$ and $Ca(OH)_2$ and TiO_2 equal to 0.1 or 0.05 *m* at 433 and 473 K. The pH of the solution was adjusted according to Table 2 using the computed amounts of KOH or NaOH to ensure a 100% phase-pure product. The amounts of the mineralizers were chosen to cover the complete pH range indicated by the yield diagram. The reaction time was adjusted to 66 h to ensure that equilibrium is achieved. Preparation of precursor solutions and charging the autoclaves were performed under either air or nitrogen atmosphere, in the latter case using a glovebag (Instruments for Research and Industry, I^2R, Weltenham, PA, Model X-37-37). After charging, autoclaves were heated in two different fashions to examine mixing related effects. First, reactions were conducted in a quiescent fashion when unstirred reaction vessels were placed in an oven. Second, reaction vessels were heated by a close-fitting insulated heating mantle (Glas-Col, Terre Haute, IN) placed on a hot plate and magnetically stirred. It was anticipated that the use of an experimental setup with stirring was important for the synthesis of $CaTiO_3$ because the reaction might be impeded by the precipitation of the sparingly soluble $Ca(OH)_2$ (cf. dashed lines in Figure 5). The precipitation of hydroxides was not of concern for other alkaline-earth titanates.[2,4]

Powders were characterized using X-ray diffraction. The analyses were performed on a Siemens D-500 diffractometer (Siemens Analytical X-ray Instruments Inc., Madison, WI) using Ni-filtered Cu Kα radiation, divergent slit of 1°, and receiving slit of 0.05°. The chemical identity of the products was determined by comparing the experimental X-ray patterns to standards compiled by the Joint Committee on Powder Diffraction and Standards (JCPDS). The morphology of the particles was examined using scanning electron microscopy (SEM, AMRAY 1400T, Bedford, MA) and transmission electron microscopy (TEM, JEOL 100CX, Peabody, MA, 100 kV accelerating voltage). Selected area electron diffraction (SAED) analysis were performed to determine crystallinity of the obtained powders.

Results and Discussion

In agreement with theoretical predictions, phase-pure $CaTiO_3$ was obtained at the synthesis conditions that lie within the >99.995% yield area (pH > 9.1 at 433 K or pH > 8.6 at 473 K). These conditions are illustrated as solid circles in Figure 3. Table 4 lists the molalities of reactants at each temperature that were used in the experimental syntheses of $CaTiO_3$. The phase-pure product was obtained using the experimental setup with stirring and nitrogen atmosphere (cf. Table 4). Also, syntheses were attempted outside of the pure product yield area. As expected, they resulted in either a mixture of unreacted TiO_2 and $CaTiO_3$ (hollow circles in Figure 3, 7.0 < pH < 9.1 for $Ca(NO_3)_2$ or 7.0 < pH < 8.8 for $Ca(OH)_2$) or only unreacted TiO_2 (× symbols, pH < 7.0 at 433 K).

X-ray analysis of the product showed that the obtained crystals are orthorhombic (JCPDS 22–153). Figure 9 shows the morphology of the obtained particles as determined by SEM analysis. The particles are cubelike with dimensions ranging from 0.2 to 0.9 μm. It was found that the $CaTiO_3$ particles obtained from $Ca(OH)_2$ with either NaOH or KOH are about two times smaller than those obtained from $Ca(NO_3)_2$. The morphology of the particles will be further investigated in a forthcoming study. Characteristic dotted SAED patterns indicated that the particles are monocrystalline.

The effect of mixing on the practical efficiency of the synthesis was examined using two experimental setups: with or without stirring. The formation of $CaTiO_3$ is kinetically inhibited by the existence of a second solid phase, $Ca(OH)_2$. This phase exists not only when $Ca(OH)_2$ is used as a feedstock but also when $Ca(NO_3)_2$ is used in conjunction with a mineralizer. In the latter case, $Ca(OH)_2$ immediately precipitates after mixing $Ca(NO_3)_2$ with a mineralizer whereas the formation of $CaTiO_3$ is sluggish. It was found that the synthesis from crystalline precursors in an autoclave without stirring yields a mixture of $CaTiO_3$, $Ca(OH)_2$, and unreacted TiO_2, which can be easily identified by X-ray diffraction (cf. Table 4). To make sure that the existence of $Ca(OH)_2$ is the primary reason for kinetic inhibitions, hydrous gel $TiO_2 x H_2O$ was used as a more reactive source of titanium. It was determined that using the gel without stirring did not improve the results (cf.,

Table 4. Selected Experimental Conditions of Hydrothermal Syntheses of $CaTiO_3$

no.	mineralizer	m_{MINER}	additional conditions	pH_{CALC}	reaction products
			T = 433 K, Precursors $Ca(NO_3)_2{\cdot}4H_2O$ and TiO_2, m_{IN} = 0.1 mol/kg of H_2O		
1	HNO_3	0.059	glovebag, stirring, crystalline TiO_2	1.51	TiO_2
2			glovebag, stirring, crystalline TiO_2	5.47	TiO_2
3	KOH	0.252	no glovebag, no stirring, crystalline TiO_2	10.05	$CaTiO_3$, $Ca(OH)_2$, $CaCO_3$, TiO_2
4	KOH	0.254	glovebag, stirring, crystalline TiO_2	10.07	$CaTiO_3$
5	KOH	0.454	glovebag, stirring, crystalline TiO_2	10.71	$CaTiO_3$
6	KOH	0.458	no glovebag, no stirring, TiO_2 gel	10.72	$CaTiO_3$, $Ca(OH)_2$, $CaCO_3$
7	KOH	0.511	glovebag, stirring, crystalline TiO_2	10.79	$CaTiO_3$
8	KOH	0.683	no glovebag, no stirring, crystalline TiO_2	10.98	$CaTiO_3$, $Ca(OH)_2$, $CaCO_3$, TiO_2
9	KOH	0.800	glovebag, stirring, crystalline TiO_2	11.07	$CaTiO_3$
10	KOH	0.797	glovebag, no stirring, crystalline TiO_2	11.07	$CaTiO_3$, $Ca(OH)_2$, TiO_2, $CaCO_3$ traces
11	KOH	0.733	no glovebag, no stirring, TiO_2 gel	11.02	$CaTiO_3$, $Ca(OH)_2$, $CaCO_3$
			T = 473 K, Precursors $Ca(NO_3)_2{\cdot}4H_2O$ and TiO_2, m_{IN} = 0.1 mol/kg of H_2O		
12	KOH	0.300	glovebag, stirring, crystalline TiO_2	10.00	$CaTiO_3$
13	KOH	0.311	glovebag, no stirring, crystalline TiO_2	10.05	$CaTiO_3$, $Ca(OH)_2$, TiO_2, $CaCO_3$ traces
14	KOH	0.527	glovebag, stirring, crystalline TiO_2	10.49	$CaTiO_3$
15	KOH	0.694	no glovebag, no stirring, crystalline TiO_2	10.66	$CaTiO_3$, $Ca(OH)_2$, $CaCO_3$, TiO_2
16	KOH	0.933	glovebag, stirring, crystalline TiO_2	10.82	$CaTiO_3$
17	KOH	1.242	no glovebag, no stirring, crystalline TiO_2	10.97	$CaTiO_3$, $Ca(OH)_2$, $CaCO_3$, TiO_2
			T = 433 K, Precursors $Ca(OH)_2$ and TiO_2, m_{IN} = 0.1 mol/kg of H_2O		
18	HNO_3	0.200	glovebag, stirring, crystalline TiO_2	5.10	TiO_2
19	HNO_3	0.131	glovebag, stirring, crystalline TiO_2	7.05	$CaTiO_3$, TiO_2
20			glovebag, stirring, crystalline TiO_2	8.01	$CaTiO_3$, TiO_2
21	KOH	0.013	glovebag, stirring, crystalline TiO_2	9.58	$CaTiO_3$, TiO_2
22	NaOH	0.064	glovebag, stirring, TiO_2 gel	10.20	$CaTiO_3$
23	NaOH	0.068	glovebag, stirring, crystalline TiO_2	10.23	$CaTiO_3$
24	KOH	0.071	glovebag, no stirring, crystalline TiO_2	10.25	$CaTiO_3$, $CaCO_3$, TiO_2
25	NaOH	0.093	glovebag, stirring, crystalline TiO_2	10.35	$CaTiO_3$

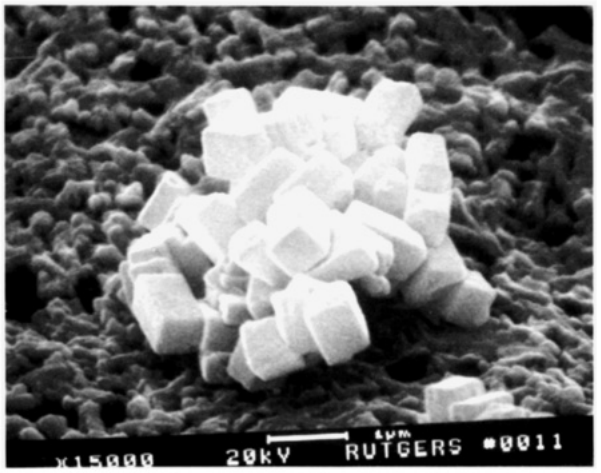

Figure 9. SEM photographs of the obtained $CaTiO_3$ powders (Table 4, reaction 9).

Table 4, reactions 6 and 11). Thus, it became evident that stirring is essential for the practical synthesis of $CaTiO_3$. When stirring is employed, the phase-pure product is obtained irrespectively of whether crystalline or hydrous TiO_2 are used as titanium sources. Since fine crystalline TiO_2 is commercially available, it is convenient source of titanium.

In comparison with the synthesis of $BaTiO_3$ and $SrTiO_3$,[2,4] the synthesis of $CaTiO_3$ is the only one that requires stirring for its practical execution. In particular, $Ba(OH)_2$ is always sufficiently soluble in water to eliminate the risk of the precipitation of solid $Ba(OH)_2$. In the case of the Sr–Ti system, the solution may become saturated with respect to $Sr(OH)_2{\cdot}8H_2O$ at temperatures below 350 K.[4] For example, $Sr(OH)_2{\cdot}8H_2O$ starts to precipitate at $m_{Sr_{IN}} = 0.10$ at 298 K, whereas $Sr(OH)_2$ precipitates at $m_{Sr_{IN}} = 0.82$ at 363 K. The solubility of strontium hydroxide octahydrate increases with temperature while the solubility of strontium hydroxide decreases. The solubility of $Ca(OH)_2$ is always low and decreases with temperature[9] as shown in Figure 5. For example, $Ca(OH)_2$ starts to precipitate at $m_{Ca_{IN}} = 0.02$ at 298 K, $m_{Ca_{IN}} = 0.01$ at 363 K, and $m_{Ca_{IN}} = 4.4 \times 10^{-3}$ at 433 K. Thus, the solubility of strontium hydroxide in either form is between 1 and 2 orders of magnitude higher than that of $Ca(OH)_2$. Therefore, stirring is not necessary in the Sr–Ti hydrothermal system. The low solubility of $Ca(OH)_2$ causes the reaction to be controlled by the transport of Ca species from hydroxide crystals to an interface bearing reactive Ti species. A shortage of Ca species near the

(9) Seidell, A. *Solubilities of Inorganic and Metal Organic Compounds*, 3rd ed.; D. Van Nostrand: New York, 1940; Vol. 1.
(10) Barin, I. In collaboration with: Sauert, F.; Schultze-Rhonhof, E.; Shu Sheng, W. *Thermochemical Data of Pure Substances*; VCH Publishers: New York, 1989, 1993.
(11) McLune, W. F., Ed. *Powder Diffraction File: Inorganic Phases*; JCPDS International Centre for Diffraction Data 1989, Swarthmore, PA, 1989.
(12) Johnson, J. W.; Oelkers, E. H.; Helgeson, H. C. *SUPCRT92: A Software Package for Calculating the Standard Molal Thermodynamic Properties of Minerals, Gases, Aqueous Species, and Reactions from 1–5000 bars and 0° to 1000°C*; University of California, Berkeley and Lawrence Livermore National Laboratory: Berkeley, 1991.
(13) Shock, E. L.; Helgeson, H. C. *Geochim. Cosmochim. Acta* **1988**, *52*, 2009.
(14) Shock, E. L.; Helgeson, H. C.; Sverjensky, D. A. *Geochim. Cosmochim. Acta* **1989**, *53*, 2157.
(15) CODATA Series on Thermodynamic Properties *CODATA Thermodynamic Tables: Selection for Some Compounds of Calcium and Related Mixtures: A Prototype Set of Tables*; Garvin, D., Parker, V. B., White, H. J., Jr., Eds.; Hemisphere Publishing: New York, 1989.
(16) Robie, R. A.; Hemingway, B. S.; Fisher, J. R. *Thermodynamic Properties of Minerals and Related Substances at 298.15 K and 1 Bar (10^5 Pascals) Pressure and at Higher Temperatures. U.S. Geological Survey Bulletin 1452*; U.S. Government Printing Office: Washington, DC, 1979.
(17) Medvedev, V. A.; Bergman, G. A.; Gurvich, L. V.; Yungman, V. S.; Vorobiev, A. F.; Kolesov, V. P. *Thermal Constants of Substances*; Glushko, V. P., Ed.; VINITI: Moscow, 1965–82; Vols. 1–10.
(18) ProChem Software: Electrochem, V. 9.0, OLI Systems Inc., Morris Plains, NJ, 1992.
(19) Baes, Ch. F., Jr.; Mesmer, R. E. *Am. J. Sci.* **1981**, *281*, 935.
(20) Chen, C. M.; Aral, K.; Theus, G. *Computer-Calculated Potential pH Diagrams to 300°, Handbook of Diagrams*; EPRI in association with Babcock & Wilcox Company: Alliance, OH, 1983; Vol. 2.
(21) Reid, R. C.; Prausnitz, J. M.; Poling, B. E. *The Properties of Gases and Liquids*, 4th ed.; McGraw-Hill: New York, 1987.

Ti interface will halt the reaction. This effect is not likely to occur in other systems such as Sr–Ti and Ba–Ti, because a higher concentration of Sr^{2+} ($SrOH^+$) or Ba^{2+} ($BaOH^+$) will render other reaction steps rate-determining (e.g., TiO_2 dissolution). In case of the Ca–Ti hydrothermal system, stirring speeds up dissolution, and this increases the flux of Ca species to the Ti interface. Stirring-assisted dissolution has been noted in many systems for precipitation with particles sizes greater than 10 μm.[22] It is likely that this is the case for the Ca–Ti hydrothermal system.

Temperature has a limited effect on the synthesis in the investigated temperature range (cf. Table 4, $T = 433$ and 473 K). Since the solubility of $Ca(OH)_2$ decreases with temperature (cf. Figure 5), higher temperatures facilitate the precipitation of $Ca(OH)_2$. However, this adverse effect is offset by the faster $CaTiO_3$ synthesis kinetics resulting from higher temperatures. Again, it should be underscored that vigorous stirring is necessary for the formation of $CaTiO_3$ in a reasonable amount of time. Another factor that affects the kinetics of the formation of $CaTiO_3$ is the particle size of TiO_2 when crystalline TiO_2 precursor is used. Since the TiO_2 particles used in our syntheses were fairly small (about 0.03 μm), the same results were obtained by using crystalline TiO_2 and the hydrous TiO_2 gel (cf. Table 4, reaction number 22). It is possible that the use of large TiO_2 particles may lead to an incomplete reaction due to sluggish kinetics.[5–8] Although the threshold particle size for crystalline titanium dioxide is not known, it has been previously determined[23] that TiO_2 with a particle size of 0.03 μm is sufficiently reactive whereas TiO_2 with a particle size of 0.18 μm is not.

In agreement with the theoretical predictions, the system Ca–Ti proved to be very vulnerable to contamination with carbonates. Indeed, whenever the solutions were prepared in contact with atmosphere, the obtained products contained appreciable amounts of $CaCO_3$ (Table 4, reactions number 3, 6, 8, 11, 15, 17) as determined by X-ray diffraction (JCPDS 5-586). According to our calculations (cf. Table 3) this is caused by the absorption of CO_2 in the high alkaline precursor solutions (both $Ca(OH)_2$ and $Ca(NO_3)_2$ + alkaline mineralizer) that are necessary for the precipitation of phase-pure $CaTiO_3$. Thus, it is necessary to prepare the solutions in a glovebag in nitrogen atmosphere. In practical syntheses, the products can be contaminated with trace amounts of $CaCO_3$ even though the reactions were carried out in a glovebag (Table 4, reactions 10 and 13). This is caused by the existence of trace amounts of $CaCO_3$ in $Ca(OH)_2$ precursors even when reagents are of the highest purity (>98.8%). Also, if the reaction products contain $Ca(OH)_2$ the mechanical manipulation of the samples in air (e.g., for X-ray analyses) leads to the absorption of CO_2 by solid $Ca(OH)_2$ in air (Table 4, reaction number 24). In principle, $CaCO_3$ could be removed from the final powder by washing with a weak acid. However, any $CaTiO_3$ synthesis that leads to the formation of small amounts of $CaCO_3$ could also produce some residual amounts of unreacted TiO_2. Since TiO_2 cannot be easily removed, a preferred synthesis route should always minimize the probability of formation of $CaCO_3$.

In general, the selection of the Ca precursor should be based on its purity provided that the synthesis is carried out in nitrogen atmosphere and with very pure mineralizers. Since in our experiments $Ca(NO_3)_2$ was purer, it was also the preferable source of calcium.

Conclusions

Thermodynamic modeling has allowed us to predict the optimum conditions for the hydrothermal synthesis of $CaTiO_3$ as well as other alkaline-earth titanates. Phase-pure $CaTiO_3$ has been synthesized using simple reagents (i.e., crystalline TiO_2 and $Ca(OH)_2$ or $Ca(NO_3)_2$) at moderate temperatures (433–473 K) in a simple experimental apparatus. While determining optimum reaction conditions, modeling studies have uncovered mechanistic sources of incomplete reaction (e.g., $Ca(OH)_2$ dissolution) as well as the effects of atmospheric contaminations. This ultimately leads to a preferred choice of calcium precursors as well as a nitrogen-processing atmosphere.

Acknowledgment. We gratefully acknowledge the generous support of the Material Division (Code 1131) at the Office of Naval Research (ONR) under the auspices of the ONR Young Investigator Program. The authors thank Ms. Lynda Renomeron for her assistance for the experimental syntheses of the powders, Dr. James O. Eckert, Jr., for assisting with the stirring setup, and John Oliver for preparing the SEM pictures.

CM940264I

(22) Nielsen, A. E. *Croat. Chem. Acta* **1980**, *53*, 255.
(23) Fajardie, F.; Lencka, M. M.; Vilmin, G.; Riman, R. E., unpublished data.